Polymer(Korea), Vol. 38, No. 1, pp. 16-23
http://dx.doi.org/10.7317/pk.2014.38.1.16

ISSN 0379-153X(Print)
ISSN 2234-8077(Online)

Orthogonal 방법을 통한 Poly(AM-DMDAAC)/MMT 고흡수성 나노복합체 제조 연구

Ming Zhou*,**, Shuangqiao Yang*,***,†, Yongguo Zhou****, Nan Qin*, Songtao He****, Dong Lai*, Zhongqiang Xie*, and Jundong Yuan****

*School of Material Science and Engineering, Southwest Petroleum University
**State Key Laboratory of Oil and Gas Reservoir Geology and Exploitation, Southwest Petroleum University
***State Key Laboratory of Polymer Materials Engineering, Polymer Research Institute of Sichuan University
****Sichuan Xinwei Rubber CO., LTD

(2013년 7월 11일 접수, 2013년 10월 1일 수정, 2013년 10월 2일 채택)

Optimization of Preparing Poly(AM-DMDAAC)/MMT Superabsorbent Nanocomposite by Orthogonal Experiment

Ming Zhou*,, Shuangqiao Yang*,***,†, Yongguo Zhou****, Nan Qin*, Songtao He****, Dong Lai*, Zhongqiang Xie*, and Jundong Yuan****

**School of Material Science and Engineering, Southwest Petroleum University, Sichuan Chengdu, 610500, China*
***State Key Laboratory of Oil and Gas Reservoir Geology and Exploitation; Southwest Petroleum University, Sichuan Chengdu, 610500, China*
****State Key Laboratory of Polymer Materials Engineering, Polymer Research Institute of Sichuan University, Chengdu 610065, China*
*****Sichuan Xinwei Rubber CO., LTD*

(Received July 11, 2013; Revised October 1, 2013; Accepted October 2, 2013)

Abstract: A novel poly(AM-DMDAAC)/MMT superabsorbent nanocomposites are prepared by radical polymerization using ammonium persulfate (APS) and anhydrous sodium sulfite as a free radical initiator and *N*,*N*-methylene bisacrylamide (MBA) as a crosslinker. In this paper, an optimization study on the synthesis of superabsorbent nanocomposites is carried out. Orthogonal array experiment indicates that the optimized conditions is acrylamide (AM) content 23 wt%, diallyl dimethyl ammonium chloride (DMDAAAC) content 6 wt%, montmorillonite (MMT) content 4 wt%, initiator content 0.2 wt% and crosslinker content 0.02 wt%. Under the optimization syntheses conditions concluded, the maximum water absorbency in distilled water is 659.53 $g \cdot g^{-1}$ and in 2 wt% sodium chloride solution is 116.25 $g \cdot g^{-1}$. Compared with the range values of different factors (R_j), the order of significance factors in distilled water is C (MMT) > B (DMDAAC) > A (AM) > D (crosslinker) > E (initiator). MMT is intercalated during polymerization reaction and a nanocomposite structure is formed as shown by TEM analysis and XRD analysis.

Keywords: superabsorbent nanocomposite, orthogonal experiment, MMT, synthesis.

Introduction

Superabsorbents are slightly crosslinked networks of flexible polymers which can absorb a great many water and swell to several times to their initial volume but do not dissolve in aqueous media. Generally speaking, large volumes of aqueous fluids can be absorb and retain by superabsorbents compared with general water absorbing materials in which the absorbed water is hardly removable even under certain heating and pressure. Due to their excellent characteristics that highly water absorbency, superabsorbents have attracted continuous interests and found potential applications in varieties industrial fields such as personal hygienic products,[1] controlled release carrier of drug,[2] petrochemical, agriculture and horticulture.[3-6]

However, the higher production cost, low water absorbency in salt solution and low gel strength of these superabsorbents limit their application widely. So how to enhance those prop-

†To whom correspondence should be addressed.
E-mail: 757903659@qq.com

erties became researchers' focus. To solve this problems, recent years, organic-inorganic superabsorbent nanocomposites which derive from the modification of organic polymer by inorganic clays have attracted great interests and attention because such materials frequently show improve performance and low production cost by intercalated and exfoliated clay-polymer composites produced.[7,8]

In this study, diallyl dimethyl ammonium chloride (DMDAAC) is used as a kind of hydrophilic cationic monomer which can copolymerize with acrylamide (AM) to generate synergic effect to enhance the water absorbency of polymer. Montmorillonite (MMT) is added to form superabsorbent nanocomposites,[9] in order to improve the heat resistance and strength of absorbent resin further. The traditional method of investigating organic-inorganic superabsorbent nanocomposites reported is single factor experiment which is very time consuming. But in this paper orthogonal array experiment is applied which is useful and powerful to optimize the preparation of poly(AM-DMDAAC)/MMT nanocomposites and evaluate their properties. Orthogonal array experiment has proven to be a cost-effective optimization strategy that can obtain the optimal conditions of each parameter in a limited number of experimental trials.

Experimental

Materials. Acrylamide (AM) and diallyl dimethyl ammonium chloride (DMDAAC), analytical grade, purified by recrystallization; Anhydrous sodium sulfite and ammonium persulfate, analytical grade, purified by recrystallization; *N*,*N*-methylene-bisacrylamide (MBA), chemical grade, purified by recrystallization; montmorillonite (MMT), industrial grade, milled and passed through a 320-mesh screen (sessile diameter 3 cm, heighten 2.5 cm, aperture 0.050 mm) prior to use; sodium chloride (NaCl), analytical grade.

Preparation of Poly(Am-DMDAAC)/Nanocomposites. According to the orthogonal table, MMT was dispersed in distilled water in a 125 mL vial and stirred on the magnetic stirring apparatus for 30 min. The copolymerization monomer AM and DMDAAC were dissolved in the above solution. The solution was heated to 37 ºC and stirred continuously until the system become homogeneous. Then, crosslinker MBA, initiator ammonium persulfate and sodium sulfite were added separately and finally the whole system weight was 50 g. In the next step, the temperature was maintained in 37 ºC for 30 min to complete the polymerization. After cooling the products to room temperature, the obtained gels were dried to constant weight at 80 ºC, and the dried gels were ground and passed through 40 to 80 mesh sieve.

Measurement of Equilibrium Water Absorbency. All groups of dried samples were immersed in excess of aqueous solutions at room temperature for 24 h to achieve swelling equilibrium. Removed swollen samples from extra water with a 100-mesh stainless screen and hanged under gravity until there were no water dropping from their surface, and then all the samples were weighted. Water absorbency (Q, g·g^{-1}) of the superabsorbent in distilled water was calculated using the following equation:

$$Q = \frac{(m_2 - m_1)}{m_1} \quad (1)$$

where, m_1 and m_2 were the weights of the dried sample and the swollen sample, respectively.

Water absorbencies in 2 wt% NaCl solution were tested according to the same procedure.

Orthogonal Arry Experimental Design. In the present investigation, the experiments are based on an orthogonal array experiment where the following five variables are analyzed: AM content (factor A), DMDAAC content (factor B), MMT content (factor C), crosslinker content (factor D) and initiator content (factor E). Based on different variables, the level of importance of each optimal condition is very different, which reported in other studies.[10] These variables which listed in Table 1 are identified to have larger effects on the water absor-

Table 1. Levels and Factors of Orthogonal Array Experiment **(unit: wt%)**

Level	Factors				
	A (AM)	B (DMDAAC)	C (MMT)	D (crosslinker)	E (initiator)
1	16	2	2	0.02	0.12
2	20	4	4	0.03	0.16
3	24	6	8	0.04	0.2
4	28	8	12	0.05	0.24

bency in distilled water and in salt solution. Therefore, the levels of factors are restricted in the present study in order to obtain optimized combination. The considered factors and levels is assigned by an L_{16} (4^5) array which is an orthogonal array of five factors and four levels just as shown in Table 1. Data analysis is carried out through the range analysis to reflect the optimal reaction conditions and their magnitudes.[11] The optimal conditions are obtained, after the orthogonal experiments and subsequent data analysis.

Range Analysis. K_{ji} and R_j are two important parameters in a range analysis. K_{ji} is defined as the sum of the evaluation indexes of all levels (i, i = 1, 2, 3, 4) in each factor (j, j = A, B, C, D, E). $\overline{K}_{ij}$ (mean value of K_{ji}) is used for evaluating the optimal level and the optimal combination of factors. When K_{ji} is the largest value, the optimal level could be obtained for each factor. R_j is defined as the range between the maximum and minimum value of K_{ji}. R_i is used to determine the effects of the factors and larger R_j means a greater effect of the factor.[12] For example, taking the L_{16} (4^5) array, the calculation is shown below[13]:

For the factor of B:

$$K_{B1} = Y_1 + Y_5 + Y_9 + Y_{13};$$
$$K_{B2} = Y_2 + Y_6 + Y_{10} + Y_{14};$$
$$K_{B3} = Y_3 + Y_7 + Y_{11} + Y_{15};$$
$$K_{B4} = Y_4 + Y_8 + Y_{12} + Y_{16};$$

$$\overline{K_{B1}} = \frac{K_{B1}}{4} \quad (2)$$

$$\overline{K_{B2}} = \frac{K_{B2}}{4};\ \overline{K_{B3}} = \frac{K_{B3}}{4};\ \overline{K_{B4}} = \frac{K_{B4}}{4}$$

$$R_j = \max(\overline{K_{Bi}}) - \min(\overline{K_{Bi}})$$

Where Y_i is the value of the result of the trial No. i; K_{Bi} is the K value of the i level of the factor of B; Other K values of the factors can be ascertained by the same calculation steps.

Characterization. TEM observation was performed in a transmission electron microscope (JEOL, model JEM 1400), applying an accelerating voltage of 80 kV. Thermal stability studies of dry samples were performed on a Perkin–Elmer TGA-7 thermogravimetric analyzer over a temperature range of 30-600 ºC, with a heating rate of 5 ºC/min and under a nitrogen flow rate of 50 mL/min. XRD patterns were obtained from an Philips PW1710 BASED X-ray diffractometer (Philips, Netherlands) (CuKα radiation, 40 kV, 30 mA). The FTIR of superabsorbent composite were recorded on a Nicolet NEXUS 360 (Nicolet, USA) spectrometer with KBr disk in the range of 4000-400 cm^{-1}.

Results and Discussion

Orthogonal Experiment in Distilled Water and NaCl Solution. Sixteen trials are carried out according to the orthogonal array experiment, and their results are shown in Table 2. This table shows that the range of the water absorbency in distilled water varies from 79.97 to 659.53 $g \cdot g^{-1}$ and in 2 wt% NaCl solution varies from 20.00 to 116.25 $g \cdot g^{-1}$, respectively. The mean values of K (K_{ji}) for different factors at different levels in the range analysis about water absorbency in distilled water and 2 wt% NaCl solution are also shown in Table 2. For each factor, as mentioned before, a higher mean value (K_{ji}) indicates that the level has a larger effect on water absorbency. Therefore, the best level for each factor can be obtained according to the highest mean value of the experimental condition (K_{ji}). According to the orthogonal array experiment, the

Table 2. L_{16} (4^5) Array and Experiment Results

Trial No.	Factors					Results (water absorbency Y_i)	
	A	B	C	D	E	Distilled water	NaCl solution
1	1	1	1	1	1	154.18	43.64
2	1	2	2	2	2	299.25	57.50
3	1	3	3	3	3	189.59	52.19
4	1	4	4	4	4	151.94	26.38
5	2	1	2	3	4	140.30	41.18
6	2	2	1	4	3	234.39	31.83
7	2	3	4	1	2	208.19	50.40
8	2	4	3	2	1	300.87	33.33
9	3	1	3	4	2	70.68	20.00

Table 2. Continued

Trial No.	Factors					Results (water absorbency Y_i)	
	A	B	C	D	E	Distilled water	NaCl solution
10	3	2	4	3	1	94.03	22.50
11	3	3	1	2	4	520.55	48.69
12	3	4	2	1	3	659.53	116.25
13	4	1	4	2	3	79.97	21.88
14	4	2	3	1	4	178.88	34.74
15	4	3	2	4	2	267.47	29.17
16	4	4	1	3	1	274.57	37.66
$\overline{K_{j1}}$	198.74	111.28	295.92	300.19	205.91		
$\overline{K_{j2}}$	220.94	201.64	341.64	300.16	211.40		
$\overline{K_{j3}}$	336.19	296.45	185.00	174.62	290.87		
$\overline{K_{j4}}$	200.22	177.27	133.54	181.12	247.92		
R_j	137.45	185.17	208.10	125.57	84.95		
Optimal condition	$A_3B_3C_2D_1E_3$						
$\overline{K_{j1}}''$	44.93	31.67	40.46	61.26	34.28		
$\overline{K_{j2}}''$	39.19	36.64	61.02	40.35	39.27		
$\overline{K_{j3}}''$	51.86	45.11	35.07	38.38	55.54		
$\overline{K_{j4}}''$	30.86	29.77	30.29	37.75	37.75		
R_j''	21.00	15.34	30.74	23.51	21.25		
Optimal condition	$A_3B_3C_2D_1E_3$						

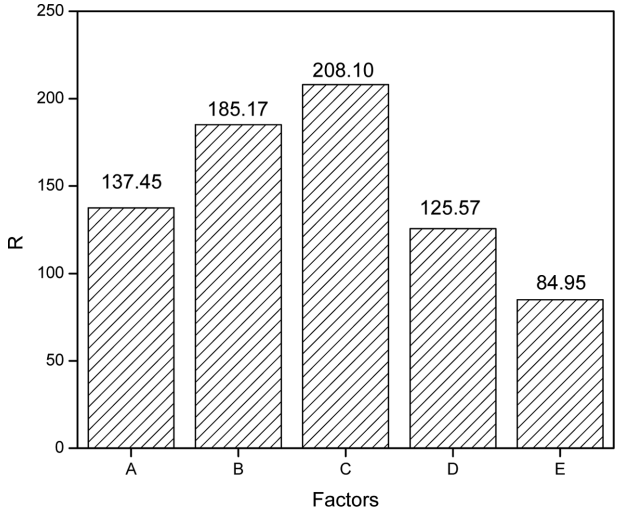

Figure 1. Range values of different factor of water absorbency.

optimized conditions of preparing poly(AM-DMDAAC)/MMT superabsorbent nanocomposite is AM content 24 wt%, DMDAAAC content 6 wt%, MMT content 4 wt%, initiator content 0.2 wt% and crosslinker content 0.02 wt%, since K_{ji} is the highest at these combinations ($A_3B_3C_2D_1E_3$) both in water absorbency and salt absorbency. As mentioned before, the range value (R_j) indicates the significance of the factor's effect on water absorbency and a larger R_j means the factor has a bigger effects on water absorbency. Therefore, compared with the range values of different factors (R_j), the factors' levels of significance are as follows: C (MMT) > B (DMDAAC) > A (AM) > D (crosslinker) > E (initiator) (Figure 1).

Effects of Each Factor on Water Absorbency in Distilled Water. The mean values of each factor are shown in Figure 2, which include five factors: A (AM), B (DMDAAC), C (MMT), D (crosslinker) and E (initiator). Based on the change in the mean value of each factor, it is obvious that group 12 th is the optimized one, whose water absorbency is 659.53 $g \cdot g^{-1}$. All five factors are analyzed as following:

The effect of AM content on water absorbency of the MMT/P(AM-DMDAAC) superabsorbent nanocomposite is shown in Figure 2. With the increase of AM content, the water absorbency increases initially and reaches a maximum when the AM content is 24 wt%. Beyond that, the water absorbency

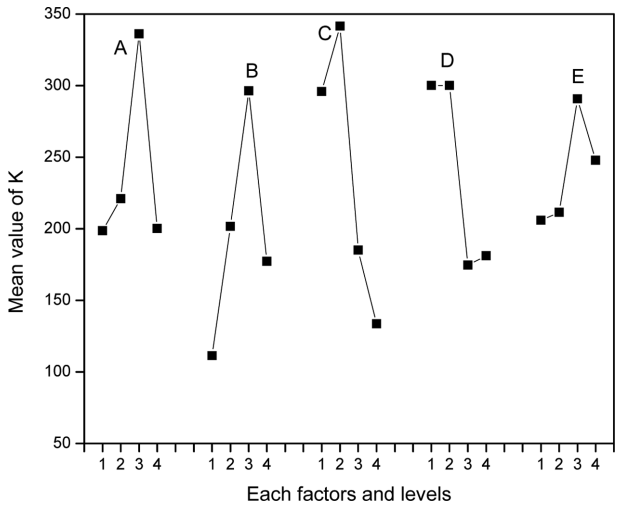

Figure 2. Relationship between water absorbency and each factors and levels.

decrease with a further increase of the AM content and the phenomenon is attributed to the following facts. When the content of AM is low, water absorbency increases with the increase of AM because AM has a positive effect on water absorbency due to its hydrophilic groups and their synergistic effect with other hydrophilic groups. But if AM content was beyond 24 wt%, the water absorbency decreases. In addition, the synergistic effect between non-ionic hydrophilic groups in AM and cationic hydrophilic groups in DMDAAC is prominent when the ration of AM to DMDAAC is in a certain range. Moreover, the water absorbency of amide group is less eminent than ionic group. Consequently, ionic group reduces with increasing content of AM, which result in the reduce of water absorbency.

The relationship between the monomer B (DMDAAC) content and water absorbency values is studied by varying the DMDAAC content from 2 to 8 wt%. As can be seen from the Figure 2, the increase of DMDAAC leads to water absorbency increase at beginning and decrease later. The reason may be that the ionic hydrophilic groups in DMDAAC contribute to their counterpart in whole network, which is positive on the ionization degree and ameliorates the resin's water absorbency to a large extend. After the content of DMDAAC is greater than 6 wt%, the excessive density of ions generates electrostatic repulsion strongly. Consequently, water absorbency of the superabsorbent nanocomposite falls when the content of DMDAAC increases further.

Figure 2 shows that with the increase of D (crosslinker content) the water absorbency increases at first and reaches a maximum when the crosslinker content is 0.03%. It is well known that the amount of crosslinking agent determined the crosslinking density of the hydrogel network. According to the theory of Flory,[14] at the lower amount of MBA, the absorbency of superabsorbent would be decreased due to the lower crosslinking density, and the stability of product will also reduce. However, the excess of MBA will cause the elasticity enhanced and the space of polymer three-dimensional network decreased, higher crosslinker content result in more crosslink points and denser networks, which prevent the network from expanding to its fullest extent and such results would not be beneficial to the swelling of product. Observations of similar phenomenon are reported previously by other researchers.[15]

The effect of the E (initiator concentration) on water absorbency is shown by Figure 2. The water absorbency increases as initiator content increasing from 0.12 to 0.2 wt% and decreases with further increase in the content of initiator. With increase of the initiator concentration, the molecular weight of the macromolecules decreases and the relative amount of polymer chain ends increase. The polymer chain ends do not contribute to the water absorbency.[16] Therefore, water absorbency decreases with increase of the initiator content. However, when the content of initiator is below 0.2 wt%, the swelling capacity of superabsorbent also decreases. This may due to a decrease in the number of radicals produced by initiator and small amount of radicals cannot guarantee the rapid crosslinking reaction. Analysis above implies that optimization content of initiator initiator is 0.2 wt%.[17]

Effects of Each Factor on Water Absorbency in 2 wt% NaCl Solution. It is very important to know the swelling behavior and water absorbency in salt solution for superabsorbent. It is well known that water absorbency decreases with increasing ionic strength of salt solutions which in this study is 2 wt% NaCl solution. This result may be the consequence of the reduction in the osmotic pressure difference between the superabsorbent and the external salt solution with increasing ionic strength. Besides, the screening effect of the additional cations on the anionic groups causes a nonperfect anion-anion electrostatic repulsion and reduces water absorbency.[18] It was our interest to investigate the water absorbency in salt solutions. As is shown in Figure 3, the optimized conditions of water absorbency in 2 wt% NaCl solution is $A_3B_3C_2D_1E_3$. Compared with the range values of different factors (R_j), the factors' levels of significance is as followed: C (MMT) > D (crosslinker) > A (AM) >E (initiator) >B (DMDAAC) (Figure 4).

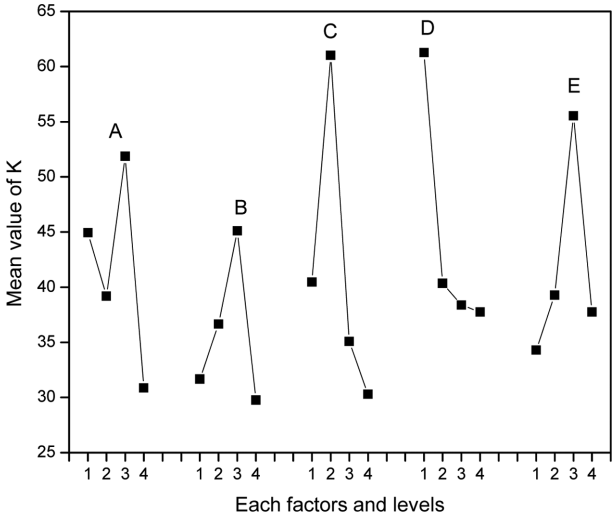

Figure 3. The relationship between salt absorbency and each factor.

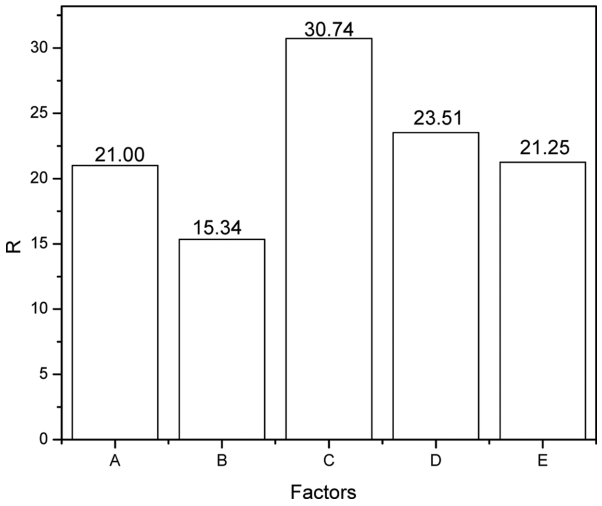

Figure 4. Range values of different factor of salt absorbency.

TEM Analysis. Figure 5 shows transmission electron microscopy (TEM) photos of poly(AM-DMDAAC)/MMT nanocomposite superabsorbent by *in-situ* intercalated polymerization. In the TEM pictures, the black filamentous content is MMT slice layer scattered in polymer matrix, and light color area is polymer matrix. MMT slice layer randomly dispersed in polymer matrix can be seen clearly from Figure 5, and length of slice layer is about 100 nm. MMT is intercalated during copolymerization reaction and a nanocomposite structure is formed as shown by TEM analysis.

Because after MMT was modified by DMDAAC, polymer molecules were connected with clay through hydrophobic hydrocarbon chain. Organic MMT was dispersed and it was packaged in the matrix of superabsorbent resin after *in-situ* intercalation-graft copolymerization. Monomers had already inserted into the nano-reactor (interlayer) of MMT, so interlayer distance increased. X diffraction peaks moved toward smaller angle, and interlayer distance (d_{001}) increased to 1.96 nm. Expanding of interlayer distance provided spatial for monomer going into interlamination in the next step. Interlayer distance (d_{001}) of dry superabsorbent resin samples was up to 2.73 nm, because copolymerization energy expanded interlayer distance of MMT.

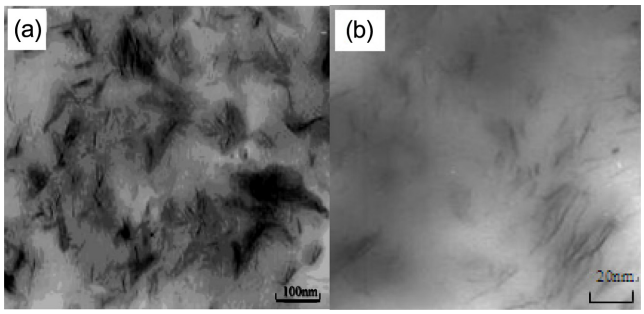

Figure 5. TEM micrograph of poly(AM-DMDAAC)/MMT superabsorbent nanocomposite. Length of slice layer are (a) 100 nm; (b) 20 nm.

Thermogravimetric Analysis. A number of works[19-21] reported thermal stability improvement for a polymer clay composite or superabsorbent composite. In this paper, the thermogravimetric analysis (TGA) of poly(AM-DMDAAC) and poly(AM-DMDAAC)/MMT containing 4 wt% MMT is carried out. As shown in Figure 6, two samples show a very small weight loss below 90 °C, which might be due to loss of

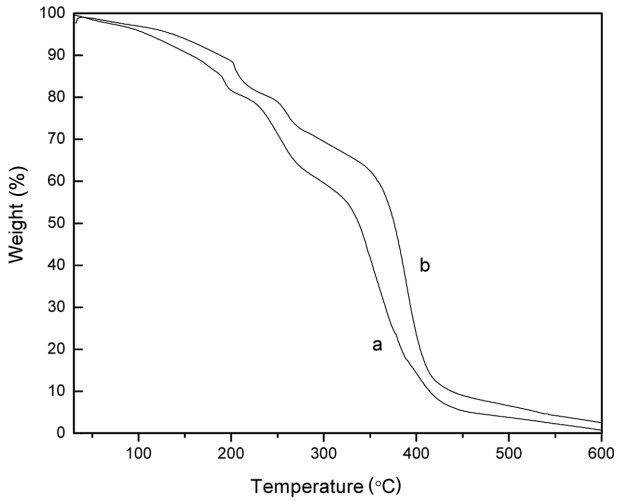

Figure 6. TGA curves of (a) poly(AM-DMDAAC); (b) poly(AM-DMDAAC)/MMT.

absorbed water. As for poly(AM-DMDAAC), the major weight loss starts at 300 ℃ (42%), whereas the major loss weight for poly(AM-DMDAAC)/MMT starts at 350 ℃ (38%). Thus, the decomposition temperature of poly(AM-DMDAAC)/MMT are higher than poly(AM-DMDAAC). The result indicates that the introduction of MMT can improve the thermal stability and this phenomenon ascribes to the dispersed clay platelets which can prevent thermal decomposition process, as a result of the barrier effect of MMT.

XRD Analysis. The change of the clay interlayer distance can be detected by XRD. XRD patterns of three structure MMT can be seen in Figure 7. The basal spacing of each sample was calculated using Bragg's law:

$$2d \sin\theta = n\lambda \quad (n = 1,\ \lambda = 1.54\ \text{Å}) \tag{3}$$

where d is the basal spacing (A°), θ is the angle of diffraction (°), λ is the wavelength (nm), and n is the path differences between the reflected waves which equals an integral number of wavelengths (λ).

The interlayer distance (d_{001}) of MMT organic MMT and poly(AM-DMDAAC)/MMT superabsorbent nanocompsite is 1.08 nm (a curve, $2\theta = 8.2°$), 1.92 nm (b curve, $2\theta = 4.6°$) and 4.01 nm (c curve, $2\theta = 2.2°$), respectively. In organic MMT, hydrated inorganic cations in clay mineral interlayer could be also replaced by various organic cations through ion exchange reaction, in other words, Na+ is replaced by quaternary ammonium cationic in HTMAB. Because after MMT is modified by DMDAAC, polymer molecules are connected with clay through hydrophobic hydrocarbon chain. Organic MMT is dispersed and it is packaged in the matrix of superabsorbent resin after *in-site* intercalation-graft copolymerization. Monomers have already inserted into the nano-reactor (interlayer) of MMT, so interlayer distance increases. X diffraction peaks moved toward smaller angle, and interlayer distance (d_{001}) increases to 1.96 nm. Expanding of interlayer distance provides spatial for monomer going into interlamination in the next step. Interlayer distance (d_{001}) of dry superabsorbent resin samples is up to 4.01 nm, because copolymerization energy expands interlayer distance of MMT, even damages its ordered structures further; exfoliated structure is formed in the superabsorbent composite. Interlayer distance (d_{001}) of dry starch grafting AM-AA/MMT superabsorbent nanocomposite is 2.73 nm in ZHOU's research,[8] so the crystal interlayer superabsorbent nanocompsite is larger than that of starch grafting AM-AA/MMT superabsorbent nanocomposite, which indicate that the exfoliation degree of crystal sheets in poly(AM-DMDAAC)/MMT superabsorbent nanocompsite increases.

Result indicates that MMT intercalated into layers of MMT and formed an intercalate nanostructure and an exfoliated nanostructure.

FTIR Analysis. The FTIR spectra of (a) poly(AM-DMDAAC) and (b) poly(AM-DMDAAC)/MMT are shown in Figure 8. In the spectrum of (a) poly(AM-DMDAAC), the absorption bands at 3410.63, 3178.34, 2925.31, 1656.03, 1403.00 and 1129.24 cm^{-1} are ascribed to -OH stretching vibration of moisture, $-NH_2$ stretching vibration of AM, $-CH_3$ stretching vibration of DMDAAC, C=O stretching vibration of AM, C-H bending vibration of AM and DMDAAC, C-N stretching vibration of DMDAAC and AM, respectively. However, for (b) poly(AM-DMDAAC)/MMT, the absorption band at 1037.98 cm^{-1} appear, which is attributed to Si-O stretching

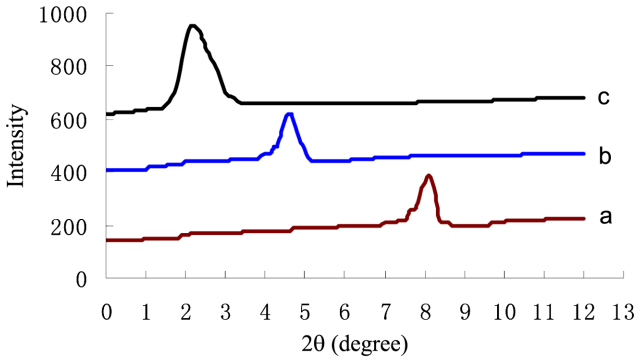

Figure 7. XRD patterns of (a) pure MMT; (b) organic MMT; (c) poly(AM-DMDAAC)/MMT superabsorbent nanocomposite.

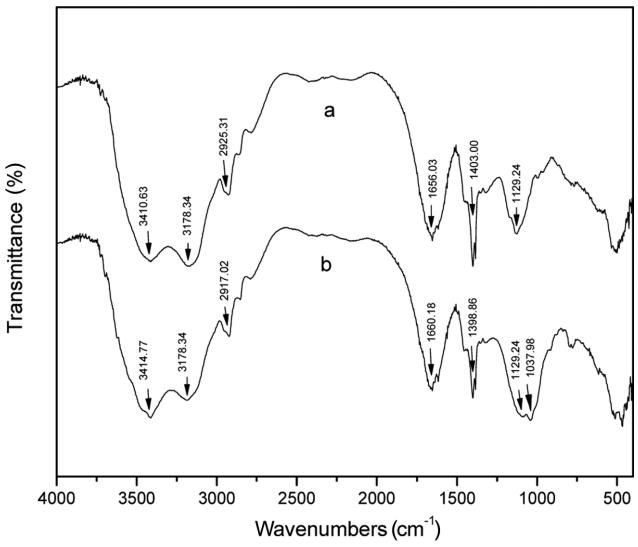

Figure 8. FTIR spectra of (a) poly(AM-DMDAAC); (b) poly(AM-DMDAAC)/MMT.

vibration of MMT. Also, the absorption band at 3414.77 cm^{-1} strengthened, which may due to the stretching bond of OH in MMT. The results indicated that the polymerization should occur between the OH groups on the surface or edge of MMT and the chains of poly(AM-DMDAAC).

Conclusions

A novel poly(AM-DMDAAC)/MMT superabsorbent nanocomposite was synthesized by copolymerization reaction of AM and DMDAAC in the presence of MMT powder in aqueous solution. The optimized conditions of preparing poly(AM-DMDAAC)/MMT superabsorbent nanocomposite is acrylamide (AM) content 23 wt%, diallyl dimethyl ammonium chloride (DMDAAAC) content 6 wt%, montmorillonite (MMT) content 4 wt%, initiator content 0.2 wt% and crosslinker content 0.02 wt%. The superabsorbent composite synthesized under optimal synthesis conditions exhibited absorption of 659.53 and 116.25 g H_2O/g sample in distilled water and in 2% NaCl solution, respectively. TEM and XRD analysis indicated that monomers intercalate layer of MMT, MMT is exfoliated during polymerization reaction and form nanocomposite structure.

This new approach showed promising in utilizing natural resource such as MMT in the production of superabsorbent material, which could significantly reduce the production cost. Also, this novel superabsorbent nanocomposite with excellent temperature-resistance properties could be especially useful for profile modification and plugging water in high temperature oil reservoir.

Acknowledgements: The authors would like to acknowledge the support of Sichuan Province higher education key laboratory of oil and gas field materials (Project No. 12YQT004).

References

1. K. Kosemund, H. Schlatter, J. L. Ochsenhirt, E. L. Krause, D. S. Marsman, and G. N. Erasala, *Regul. Toxicol. Pharm*., **53**, 81 (2009).
2. M. Sadeghi and H. Hosseinzadeh, *J. Bioact. Compat. Pol*., **23**, 381 (2008).
3. M. Zhou, Y. Yang, and J.-L. Dai, *Polym. Mater. Sci. Eng. (Chinese)*, **24**, 36 (2008).
4. R. Po, *J. Macromol. Sci. Rev. Macromol. Chem. Phys*., **C34**, 607 (1994).
5. J. Zhang, K. Yuan, Y.-P. Wang, S.-J. Gu, and S.-T. Zhang, *Mater. Lett.*, **61**, 316 (2007).
6. T. Wan, X. Q. Wang, Y. Yuan, and W. Q. He, *J. Appl. Polym. Sci*., **102**, 2875 (2006).
7. A. Q. Wang and J. P. Zhang, *Organic/Inorganic Superabsorbent Composites (Chinese)*, Science, Beijing, 2006.
8. M. Zhou, J.-Z. Zhao, and L.-Z. Zhou, *J. Appl. Polym. Sci*., **121**, 2406 (2011).
9. L. B. de Paiva, A. R. Morales, and F. R. V. Díaz, *Appl. Clay Sci*., **42**, 8 (2008).
10. K. Y. Chan, C. K. Kwong, and X. G. Luo, *Expert. Syst. Appl.*, **36**, 7379 (2009).
11. H. Evangelaras, E. Kolaiti, and C. Koukouvinos, *J. Stat. Plan. Infer.*, **136**, 3698 (2006).
12. C. Chuanwen, S. Feng, L. Yuguo, and W. Shuyun, *J. Mater. Sci.: Mater. Electron*., **21**, 349 (2009).
13. W. U. Xuan and Y. C. L. Dennis, *J. Appl. Energ.*, **88**, 3615 (2011).
14. P. J. Flory, *Principles of Polymer Chemistry*, Cornell University Press, Ithaca, 1953.
15. J. W. Chen and Y. M. Zhao, *J. Appl. Polym. Sci*., **75**, 808 (2000).
16. A. Li, A. Q. Wang, and J. M. Chen, *J. Appl. Polym. Sci*., **92**, 1596 (2004).
17. M. Zhou, J.-Z. Zhao, and W.-F. Pu, *E-Polymers*, **84**, 1618 (2012).
18. B. M. Gholam, R. M. Gholam, and G. Shahrzad, *J. Polym. Res*., **18**, 1487 (2011).
19. F. S. Xue, Z. Guo, and X. J. Kun, *Polym. Bulletin*, **60**, 69 (2008).
20. M. Yadav and K. Y. Rhee, *Carbohydr. Polym.*, **90**, 165 (2012).
21. S. F. Wang, L. Shen, Y. J. Tong, L. Chen, I. Y. Phang, P. Q. Lim, and T. X. Liu, *J. Polym. Degrad. Stab*., **90**, 123. (2005).